Environmental Pollution 245 (2019) 173–182

Contents lists available at ScienceDirect

Environmental Pollution

journal homepage: www.elsevier.com/locate/envpol

Atmospheric deposition of antimony in a typical mercury-antimony mining area, Shaanxi Province, Southwest China☆

Ming Ao [a, b], Guangle Qiu [b], Chao Zhang [b], Xiaohang Xu [b], Lei Zhao [b], Xinbin Feng [b], Song Qin [a], Bo Meng [b, *]

[a] Institute of Soil and Fertilizer, Guizhou Academy of Agricultural Sciences, Guiyang, 550006, PR China
[b] State Key Laboratory of Environmental Geochemistry, Institute of Geochemistry, Chinese Academy of Sciences, Guiyang, 550002, PR China

ARTICLE INFO

Article history:
Received 22 August 2018
Received in revised form
29 October 2018
Accepted 29 October 2018
Available online 1 November 2018

Keywords:
Hg-Sb mining
Atmospheric deposition
Antimony
Wet and dry deposition

ABSTRACT

Mercury-antimony (Hg–Sb) mining activities are important anthropogenic sources of Hg and Sb to the local environment. The Xunyang Hg–Sb mine situated in Shaanxi Province is an active Hg mine in China. To understand the emission, transportation, and deposition of Sb through Hg–Sb mining activities, current study systematically monitored the Sb concentration in precipitation in the Xunyang Hg–Sb mining district. Five groups of experimental pots were carefully designed to further investigate the influence of Hg–Sb mining activities on the Sb contamination in the local surface soil. Based on the overtime increasing of the Sb concentrations in soil from experimental pots, for the first trial, we estimated the atmospheric deposition flux/mass of Sb in the Xunyang Hg–Sb mining district. Our results showed that the concentrations of Sb in precipitation in the Xunyang Hg–Sb mining district ranged from 0.71 μg L^{-1} to 19 μg L^{-1} (mean = 4.2 ± 4.5 μg L^{-1}), which was orders of magnitude higher than that at the control site. As expected, the concentration of Sb in precipitation was highly elevated near of the Hg–Sb smelter and gradually decreased with distance from the smelter. After 12 months exposure, Sb concentrations in soil of experimental pots were increased by 1.2–8.5 times. The average atmospheric wet and dry deposition flux of Sb in the Xunyang Hg–Sb mining district were 7.2 ± 6.9 μg m^{-2} day^{-1} and 2.1 ± 4.7 mg m^{-2} day^{-1}, respectively; the annual wet and dry deposition mass of Sb through Hg–Sb mining activities were estimated to be 1.6 t y^{-1} and 158 t y^{-1}, respectively, indicating that dry deposition was the dominant pathway (98 ± 1.2%) for the removal of Sb from the atmosphere. Our results confirmed that the ongoing Hg–Sb mining activities resulted to serious Sb contamination to terrestrial ecosystems, posing a potential threat to local residents in the Xunyang Hg–Sb mining district.

1. Introduction

Antimony (Sb) is widely present in environmental compartments (Wilson et al., 2010). Generally, concentrations of Sb in the earth's crust are estimated to be < 0.3 mg kg^{-1} (Wedepohl, 1995), and the background concentrations of Sb in soils are present in the span < 0.3–8.4 mg kg^{-1}, but it tends to be concentrated in the surface soils (Hammel et al., 2000). Sb and its compounds are recognized as hazardous to human health (i.e., carcinogenic) (Schnorr et al., 1995) and geochemically categorized as a chalcophile element, co-occurring with sulfur and other metals and metalloids, such as mercury (Hg) and lead (Pb) (Hu et al., 1996).

Similar to Hg, Sb as a global pollutant, can be transported long distances in the atmosphere (Shotyk et al., 2004; Krachler et al., 2005; Tian et al., 2014). The chemical speciation of Sb defines the bioavailability and the toxicity of this element in biological samples. For example, elemental Sb is most toxic, followed by Sb(III) compounds, and eventually species in the higher + V state (Smichowski, 2008). In turn, the general toxicity of inorganic Sb is higher than for organic Sb compounds (Kentner et al., 1995). Sb and its compounds have been considered pollutants of priority interest by several organizations, including the United States Environmental Protection Agency (USEPA) and the European Union (EU), and Sb is also on the list of hazardous substances under the Basel convention concerning the restriction of transfer of hazardous waste across borders (Filella et al., 2002). The World Health Organization set safe drinking water levels for Sb at 20 μg L^{-1} (WHO,

☆ This paper has been recommended for acceptance by Joerg Rinklebe.
* Corresponding author.
E-mail address: mengbo@vip.skleg.cn (B. Meng).

https://doi.org/10.1016/j.envpol.2018.10.125
0269-7491/

1996). In China, the maximum admissible Sb level in drinking water is 5 μg L^{-1}, and the recommended level in Japan is less than 2 μg L^{-1} (Zheng et al., 2000; He, 2007). In areas with high levels of airborne Sb, long-term inhalation of Sb particulates and soot may cause lung cancer, 'Sb pneumoconiosis', 'Sb calm disease' and other diseases (Schnorr et al., 1995). Previous studies confirmed an increase in mortality from lung cancer and feasibly ischemic heart and non-malignant respiratory disease in workers exposed to Sb, with an incubation period of up to 20 years (Jones et al., 1994; Schnorr et al., 1995).

Natural processes and anthropogenic activities can release Sb into the atmosphere. Among the former processes wind-borne dust, sea salt spray, volcanic activity, forest fires, biogenic sources are dominant, while anthropogenic sources include energy production (coal, oil and gas), mining, smelting and refining, fossil fuel combustion, waste incineration, and others (Bloch et al., 1983; Nriagu and Pacyna, 1988; Nriagu, 1989; Shotyk et al., 2004; Tian et al., 2011, 2014). The anthropogenic emissions of Sb to the atmosphere was estimated to be 3.5×10^3 t y^{-1}, which was predominant over natural sources (2.6×10^3 t y^{-1}) (Filella et al., 2002).

Previous study demonstrated that atmospheric deposition was the primary source of metals and metalloids in surface soil and aquatic ecosystems (Nriagu and Pacyna, 1988). Therefore, a systematic study concerning the influence of atmospheric deposition on soil metal pollution is not only of great theoretical value, but also of great importance in preventing and controlling metals and metalloids pollution and protecting human health, especially in mining and smelting areas. Ainsworth et al. (1990) observed a strong gradient in Sb content of soils and biota downwind a Sb smelter with maximum values of 1489 and 336 mg kg^{-1} in its proximity, respectively, which were orders of magnitude higher than the level at a rural control site (<1 mg kg^{-1}). Using pot experiments, the researchers elucidated that Sb in vegetation was largely derived from atmospheric deposition rather than by uptake from soil (Ainsworth et al., 1990). However, studies on sources, transportation, and geochemical behavior of Sb in the environment are very limited (Cloy et al., 2005; Filella et al., 2016).

China was ranked as the top producer of Sb in the world, with approximately 84% of the share globally (He et al., 2012). Mining and smelting activities have produced large amounts of waste and released large quantities of Sb into the environment (He and Yang, 1999; He, 2007; Zhang et al., 2009a), resulting in serious Sb contamination to ambient waters, soils, and sediments. For instance, the concentrations of Sb can reach up to 6384 μg L^{-1} in water samples from Chengdu City, Sichuan Province China (Wang et al., 2010). Located in midland of China, the Xikuangshan Sb mine is one of the largest Sb mines in the world; Sb concentrations in soil and sediment samples can reach up to 5045 mg kg^{-1} and 7316 mg kg^{-1}, respectively (He, 2007). Large-scale mining and smelting activities are still ongoing in the Xunyang mercury-antimony (Hg-Sb) mining district during the period from 2012 to 2013, which has resulted in metal and metalloid pollution problems, especially for Sb and Hg (Qiu et al., 2012; Zhang et al., 2009b). Previous study reported that concentration of gaseous elemental Hg (GEM) in ambient air in the Xunyang mercury-antimony mining district ranged from 7.4 to 410 ng m^{-3} (Qiu et al., 2012). The concentrations of total Hg (THg) and methylmercury (MeHg) in paddy soil in the Xunyang Hg–Sb mining district were highly elevated, reaching up to 750 mg kg^{-1} and 11 μg kg^{-1}, respectively (Qiu et al., 2012; Zhang et al., 2009b). Qiu et al. (2012) observed that the rice seed (edible portion) grown at the Xunyang Hg–Sb mining district contained THg and MeHg levels up to 200 μg kg^{-1} and 80 μg kg^{-1}, respectively. Furthermore, the concentrations of Hg in ambient air, paddy soil, and rice seed were all decreased with the increasing distance from the smelter (Qiu et al., 2012). In the Xunyang Hg–Sb mining district, Hg and Sb are symbiotic; however, only Hg is recovered in the smelting process. Mining and smelting waste gas and waste water were directly discharged into the surrounding environment; waste rocks were piled along the banks of the local river (e.g. Zhutong River in Xunyang) without any treatment. More importantly, previous studies only focused on Hg and ignored the influence of Sb on the surrounding environment in the Xunyang Hg–Sb mining district (Qiu et al., 2012; Zhang et al., 2009b).

In this study, we systematically monitored the Sb concentrations in atmospheric wet deposition during the period from June 2012 to June 2013 in the Xunyang Hg–Sb mining district. Five groups of experimental pots filled with topsoil (1–10 cm) from a control site with low level of Sb were distributed along a perceived depositional gradient from the smelter to address the emissions, transportation, and deposition of atmospheric Sb through Hg–Sb mining activities. The objectives of this study were (1) to reveal the temporal and spatial variations of atmospheric deposition of Sb from mining and smelting activities, and (2) to estimate the deposition flux and annual deposition mass of Sb in the Xunyang Hg–Sb mining district comparing the soil experiment.

2. Materials and methods

2.1. Study area

The Xunyang Hg–Sb mining district (N: 32°51′38″–33°05′23″, E: 109°23′31″–109°31′31″) is situated in Xunyang county, Shaanxi Province, Southwest China (Fig. 1). The Xunyang Hg–Sb mine is known as an important production base of Hg and Sb in China. The total reserves of Sb deposits in the Xunyang Hg–Sb mining district is estimated to be 43,656 t. The historical Hg–Sb mining activities in the Xunyang Hg–Sb mining district can be dated back to the Spring Autumn period and the Warring States period (770–221 BCE). The smelting process only treats Hg retrieving but rather than any other metals. Furthermore, huge quantities of residues from the retorting process (e.g. waste rocks and waste residue) are adjacent to local river without any treatment. The mine drainage and waste water from the calcines directly flow into the local stream water.

The Xunyang Hg–Sb mining district is a typical mountainous topography with elevations ranging from 185 m to 2358 m. It experiences a sub-tropical humid climate with an annual average rainfall of ~851 mm and a perennial mean temperature of ~15 °C. Two major rivers including Zhutong river and Shengjia river draining the study area, flow into the Shuhe River and finally into the Han River. There are two Hg–Sb mine (Qingtonggou and Gongguan) and one Hg smelting factory in the Xunyang Hg–Sb mining district (Fig. 1). The Qingtonggou Hg–Sb mine and Hg–Sb smelter are located in the upstream of Zhutong river (Fig. 1).

2.2. Experimental design and sample collection

2.2.1. Experimental sites

In this study, we evaluated the impacts of dry/wet atmospheric deposition of Sb from the Hg–Sb mining and smelting activities on the terrestrial ecological environment in the Xunyang Hg–Sb mining district. Four experimental locations which distributed among gradient atmospheric Sb deposition in the Xunyan Hg–Sb mining district, were selected as pollution sites, namely S1, S2, S3 and S4 (Fig. 1). In detail, the distance from S1 to the smelter is ~0.5 km. S2, S3 and S4 are located in the downwind direction of smelter, which are ~4.0 km, ~6.0 km, and ~12 km from the smelter, respectively (Fig. 1). Site S5 chosen as control site, is far away (~26 km) from the pollution source (smelter).

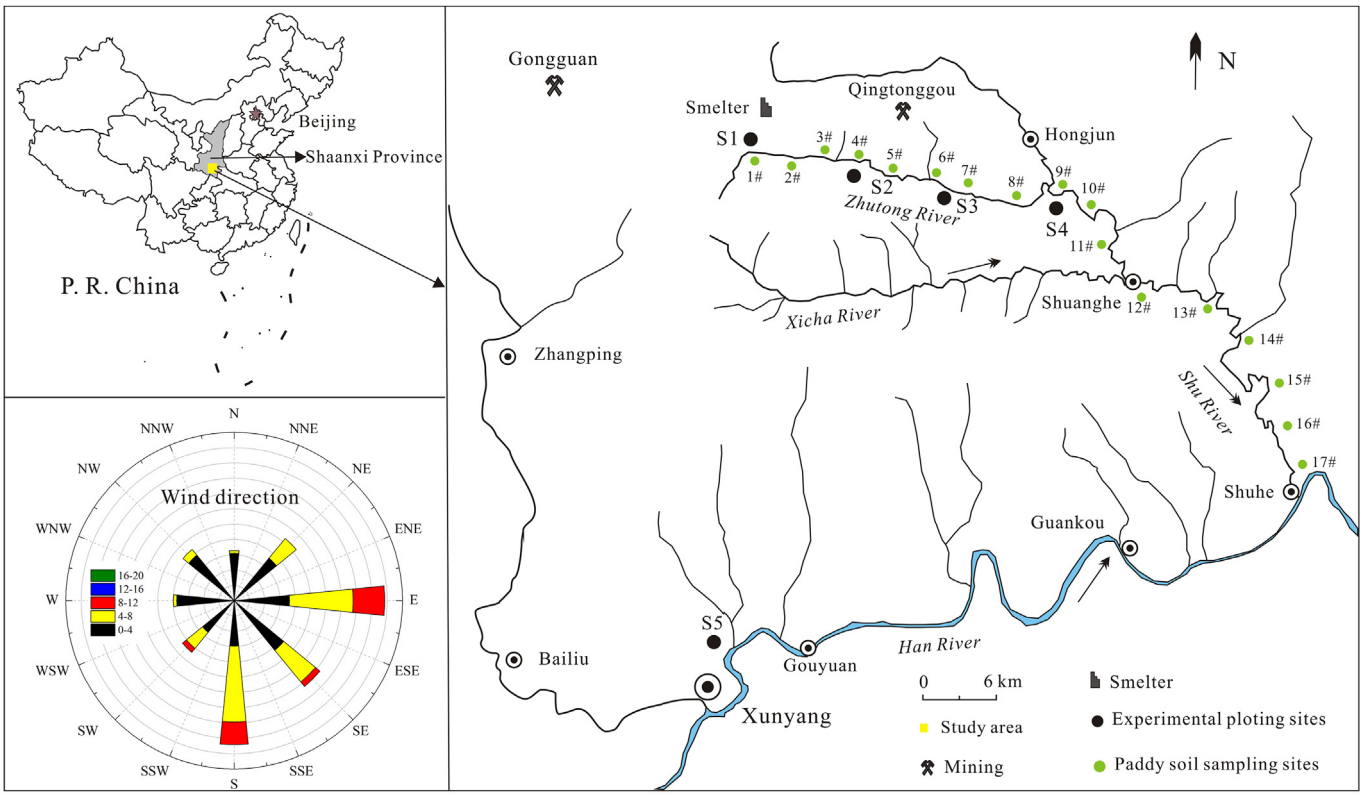

Fig. 1. Map of the study area, the sampling locations, and annual wind direction in the Xunyang Hg–Sb mining district and regional background site.

2.2.2. Experimental pots

To evaluate the influence and accumulative characteristics of both dry and wet Sb deposition through Hg–Sb mining activities on the terrestrial ecosystem, a custom-designed receiver pot of wooden box (dimension $30 \times 30 \times 40$ cm) was employed in this study. In order to avoid the loss of water and pre-deposited Sb in the experimental pots, the inside of the wooden boxes were equipped by of impermeable plastic membrane. The volume of experimental pot is ~0.036 m^3, with a receiving area of ~0.09 m^2. Three parallel pots were placed in an open space and ~1 m above the surrounding ground in order to avoid any contamination from soil particles and human activities for each of the sampling sites. Experimental pots were filled with topsoil (1–10 cm) collected from the paddy field (Huaxi, Guizhou Province, China) with a low level of Sb (3.4 ± 0.09 mg kg^{-1}). The average concentration of organic matter in soil was $5.8 \pm 0.26\%$. The topsoil from paddy field was air-dried, ground to 2 mm, and fully mixed before use. Each experimental pot was filled with 15 kg soil; the depth of the soil in the pot is ~20 cm. Finally, the soil in the pot was irrigated with the local drinking water containing a low concentration of Sb (0.75 ± 0.27 μg L^{-1}) and received atmospheric Sb deposition flux of Xunyang Hg–Sb mining district.

2.2.3. Sample collection and preparation

An integrated bulk precipitation sampler based on the design of Guo et al. (2008) was used in the field to monitor the concentration of Sb in cumulative precipitation. The sampling train consisted of three borosilicate glass components: (1) a funnel (15 cm diameter), (2) a connecting tube, acting as capillary to prevent the diffusion of ionic state elements into the precipitation sample as well as the volatilization of element from sample, and (3) a sampling bottle. The sampling device was fixed on a tripod and ~1.5 m above the ground to avoid contamination from soil particles by splashing during heavy rainfall. Previous studies confirmed that there were no statistically differences between wet-only event and manual event collection, weekly volume-weighted wet-only event and weekly bulk collection (Guentzel et al., 1995; Landis and Keeler, 1997; Landing et al., 1998; Guo et al., 2008). Furthermore, no significant differences were observed for concentrations and deposition fluxes of mercury between wet-only and monthly-integrated bulk precipitation (Landing et al., 1998; Guentzel et al., 2001; Guo et al., 2008). Therefore, it is reasonable that the cumulative precipitation samples in this study can be recognized as wet deposition only. The precipitation samples were collected monthly during the period from June 2012 to July 2013; all the sampling device was replaced after each of the sampling campaigns. It should be noted that the receiving precipitation during the period from November to February was a mixed sample since very less rainfall during winter. The unfiltered samples were poured into two 100 mL borosilicate glass bottles for total Sb analysis.

The paddy soil samples were collected along the Zhutong river in the Xunyang Hg–Sb mining district in October, 2011. In total, 17 sampling sites were selected in this study (Fig. 1). Soil samples were collected from 1 to 10 cm of the surface layer. At each sampling site, the final sample was composed of 5 sub-samples within an area of 5–10 m^2 following the diagonal sampling technique. Approximately, 0.25 kg (wet weight) of soil samples (1–10 cm depth) from experimental pots were collected once every two months during the period from August 2012 to June 2013. Totally, 6 sampling campaigns were conducted for each of the sampling locations. The soil sample was collected by hand with a disposable polyethylene glove. It should be noted that the location for each the samples is different to that of previous sampling campaigns, in order to avoid any disturbance of the soil profile in the experimental pots. Previous studies showed that Sb had less mobility in soil environments than arsenic and copper (Hammel et al., 2000; Wilson et al., 2004).

Ainsworth et al., (1990) further confirmed that Sb tended to concentrate in surface soils near smelters. Moreover, iron-aluminum oxides and iron hydroxides in soil represent high affinity with Sb, and the presence of these minerals seemed to be responsible for the high sorption capacity to Sb (Meima and Comans, 1998; Tighe et al., 2005; Nakamaru et al., 2006), which makes Sb through atmospheric deposition difficult to move vertically.

Raining water samples for total Sb analysis were acidified on-site to 0.4% (*v*/*v*) using concentrated ultrapure nitric acid; the samples bottles were then sealed, double-bagged and transported to the lab on ice within 24 h. They were stored in a refrigerator at 4 °C in the dark until analysis. Soil samples were stored in polyethylene bags to avoid cross-contamination and transported (within 24 h) in an ice-cooled container to a refrigerator kept at −18 °C prior to freeze-drying. Subsequently, the freeze-dried soil samples were homogenized to a size of 200 meshes per inch with a mortar for total Sb analysis.

2.3. Sample analyses

2.3.1. Total Sb analyses

For total Sb analysis, ~0.05 g of soil samples was placed in a PTFE crucible, and 1 mL of HNO_3 and 0.5 mL of HF were added to each sample. The crucible was sealed within a stainless-steel bomb and heated at 170 °C for 30 h. The digestion bomb was opened only after it cooled down to room temperature to avoid any loss of analyte through evaporation. The solution was heated to dryness, and 1 mL of HNO_3 was added and evaporated to dryness again. The residue was re-dissolved in 1 mL of HNO_3 and diluted to 100 mL for analysis. A suitable volume of aliquot from the digested sample was taken for total Sb analysis by inductively coupled plasma mass spectrometry (ICP-MS, Agilent 7700x, Agilent Technologies Inc., California, American). Total Sb concentration in precipitation samples was quantified using ICP-MS. All samples were analyzed at the State Key Laboratory of Environmental Geochemistry, Institute of Geochemistry, Chinese Academy of Sciences.

2.3.2. Quantifying the deposition flux and deposition mass of Sb

The monthly rainfall data in Xunyang Hg–Sb mining district was kindly provided by the local Meteorological Bureau in Xunyang county, Shannxi Province. The wet deposition fluxes of Sb were calculated using the monthly average Sb concentration data and the monthly rainfall data (Al-Momani, 2008):

$$F_w = \frac{C_i \times R_i}{\Delta T} \tag{1}$$

where F_w is the wet deposition flux of Sb (μg m^{-2} day^{-1}); C_i is the monthly average Sb concentration in precipitation (μg L^{-1}); R_i is the monthly rainfall (mm); i is the sampling period; ΔT is the time elapsed (day).

Based on the temporal concentrations of Sb in surface soil of the experimental boxes, the total (dry and wet) deposition fluxes of Sb were calculated in this study:

$$F_d = \frac{C_i \times C_{i-1}}{\Delta T} \times M - F_w \tag{2}$$

where F_d is the total deposition flux of Sb (mg m^{-2} day^{-1}); C_i is the average Sb concentration in experimental soil (mg kg^{-1}); i is the sampling period; ΔT is the time elapsed (day); M is the weight of soil (1–10 cm depth) in experimental box (7.5 kg). The dry deposition flux of Sb can be obtained by the difference between the total deposition flux and the wet deposition flux of Sb.

On the basis of the calculated wet deposition flux of Sb, we further estimated the annual wet deposition mass of Sb through the smelting factory in the Xunyang Hg–Sb mining district:

$$M_w = F_w \times \Delta A_n \times 365 \times 10^{-9} \tag{3}$$

where M_w is the annual wet deposition mass of Sb (t y^{-1}); F_w is the wet deposition flux of Sb (μg m^{-2} day^{-1}); n is the sampling site (n = S1, S2, S3, S4, S5); ΔA_n is the specific areas between the two adjacent experimental sites (m^2); and 365 is a unit conversion factor for a year. It should be noted that the study area in the Xunyang Hg–Sb mining district is divided into five sub-areas based on the locations of smelter and selected five sampling sites. The location of smelter is treated as the center of the circle; the distance between smelter and sampling site is treated as the circle radius. The specific sub-area is calculated by the area difference between the two adjacent sampling sites. For example, when n = 1, ΔA_n is the area within the S1 and the location of smelter and S1 treated as the center and radius of the circle; when n = 2, ΔA_n is the area difference between the area within S1 and S2.

Based on the temporal concentrations of Sb in surface soil of the experimental boxes, the total annual deposition mass of Sb was estimated as indicated in Ferrat et al. (2012):

$$M_t = \frac{\left(C_f - C_0\right) \times M \times \Delta A_n}{A} \times 10^{-9} \tag{4}$$

where M_t is the annual deposition mass of Sb in soil (t $year^{-1}$); n is the sampling site (n = S1, S2, S3, S4, S5); C_f is the Sb concentration in soil sample at the end of the sampling period (mg kg^{-1}); C_0 is the ambient Sb concentration in the original soil (3.4 ± 0.09 mg kg^{-1}); ΔA_n is the specific sub-area between the two adjacent experimental sites (m^2); M is the weight of soil (1–10 cm depth) in experimental box (7.5 kg); A is the area of receiving atmospheric Sb deposition (0.09 m^2). The annual dry deposition mass of Sb can be obtained by the difference between the total annual deposition mass (Eq. (4)) and the annual wet deposition mass (Eq. (3)) of Sb.

2.4. Quality control

Quality control for Sb determination in samples was performed using triplicates, method detection limits, method blank, and certified reference material. The method detection limits, based on three times the standard deviation of replicate measurement of blank solution (3 × σ), were 5.0 μg kg^{-1} for total Sb in soil sample and 9.0 ng L^{-1} for total Sb in water sample. The method blank was in each case less than the detection limit. The variability between the triplicate samples was less than 7.7% for total Sb analysis both in water samples and soil samples. The certified reference material of soil (GBW07405, National Research Center for Certified Reference Materials) was employed for quality control of soil sample analysis, with the values obtained being 38 ± 1.7 mg kg^{-1} (n = 6), which is comparable with the certified value of 35 ± 5.0 mg kg^{-1}.

Statistical analysis was performed using SPSS 11.5 software. Correlation coefficients(r) and significance probabilities (p) were computed for the linear regression fits. T-test were employed to compare significant difference in mean involve independent samples (unpaired samples) or paired samples when the data sets following normal distribution. Significant differences were all declared at $p < 0.05$.

3. Results and discussion

3.1. Concentration of Sb in precipitation

Concentrations and distribution of Sb in precipitation at four sampling sites (S1–S4) in Xunyang Hg–Sb mining district and control site (S5) are shown in Fig. 2. During the sampling period, the average (range) concentrations of Sb in precipitation at S1, S2, S3 and S4 were $7.1 \pm 4.6\ \mu g\ L^{-1}$ ($1.3–15\ \mu g\ L^{-1}$), $3.5 \pm 3.5\ \mu g\ L^{-1}$ ($0.71–12\ \mu g\ L^{-1}$), $6.6 \pm 6.5\ \mu g\ L^{-1}$ ($0.76–19\ \mu g\ L^{-1}$) and $3.1 \pm 2.0\ \mu g\ L^{-1}$ ($1.1–7.9\ \mu g\ L^{-1}$), respectively. Corresponding data was $0.65 \pm 0.49\ \mu g\ L^{-1}$ ($0.19–1.7\ \mu g\ L^{-1}$) at control site of S5. Our results showed that the Sb concentrations in Xunyang Hg–Sb mining district (S1–S4) were highly elevated and 1–2 orders of magnitude higher that in the regional background measured at S5.

The concentration of Sb in precipitation in Xunyang Hg–Sb mining district was compared with data from the literature. Concentrations of Sb in precipitation in the Xunyang Hg–Sb mining district (S1–S4) was slightly lower than that in Tangshan City ($9.4\ \mu g\ L^{-1}$, Li et al., 2012), a typical industrial city in Northern China. While the Sb concentration in precipitation at control site of S5 represented the similar level when compared with the data in urban areas worldwide, such as Chengdu City in China (ranging from 0.87 to $2.6\ \mu g\ L^{-1}$, Wang et al., 2010), urban area in Canada ($0.35 \pm 0.10\ \mu g\ L^{-1}$, Filella et al., 2002), and Greater Brisbane in Australia ($0.15 \pm 0.09\ \mu g\ L^{-1}$, Huston et al., 2012), suggesting that the control site of S5 was less impacted by the smelter in the Xunyang Hg–Sb mining district. Li et al. (2012) further indicated that steel smelting emissions, fugitive dusts, and coal combustion were principal contributions of Sb in the precipitation in Tangshan city. For the urban area, such as Chengdu City, China (Wang et al., 2010) and Greater Brisbane, Australia (Huston et al., 2012), the Sb in precipitation primarily originated from dust and fossil fuel combustion. In this study, the highly elevated Sb in precipitation at S1–S4 can be linked to the ongoing Hg–Sb smelting and mining activities in the Xunyang Hg–Sb mining district. Sb concentration in precipitation is logically reflecting the enhanced flux of atmospheric deposition of Sb.

There were seasonal variations of Sb in precipitation between rainy season (April–September) and dry season (January–March and October–December) in Xunyang Hg–Sb mining district. The Sb concentrations in Xunyang Hg–Sb mining district (S1, S2, S3 and S4) in dry season were significantly higher than that in rainy season (T-test, $p < 0.01$) (Fig. 2). On one hand, the elevated Sb concentration during dry seasons can be explained by the reducing rainfall in the Xunyang Hg–Sb mining district. It has been reported that the concentrations of constituents in precipitation generally decreases with precipitation depth during a rainfall event (Chate et al., 2003; Shimamura et al., 2006). On the other hand, the Xunyang Hg–Sb mining district is dominated by snowfall during the dry seasons especially in winter. Previous study demonstrated that the snowfall can dramatically promote Sb deposition from the air (Graedel and Franey, 1975), which could result to the relatively higher Sb in precipitation during dry season especially in winter. On the opposite, the rainfall is mainly concentrated in rainy season in the Xunyang Hg–Sb mining district. In addition the increased emission strength from coal burning in cold seasons is a major contributor (Pan and Wang, 2015). Therefore, the relatively lower Sb in precipitation in Xunyang Hg–Sb mining district during rainy season could be attributed to the dilution effect which resulted from the increased rainfall amount. Differently, the Sb concentration in precipitation in control site of S5 remained stable during the sampling periods, with slightly increased in February (no significant difference) (Fig. 2). The slightly increased Sb in February (winter) probably related to the local house heating using coal, which was an important Sb emission source to the air (Tian et al., 2011). The relatively low Sb concentrations in precipitation at S5 further indicated that the control site (S5) was less impacted by atmospheric Sb emissions from the smelter in Xunyang Hg–Sb mining district.

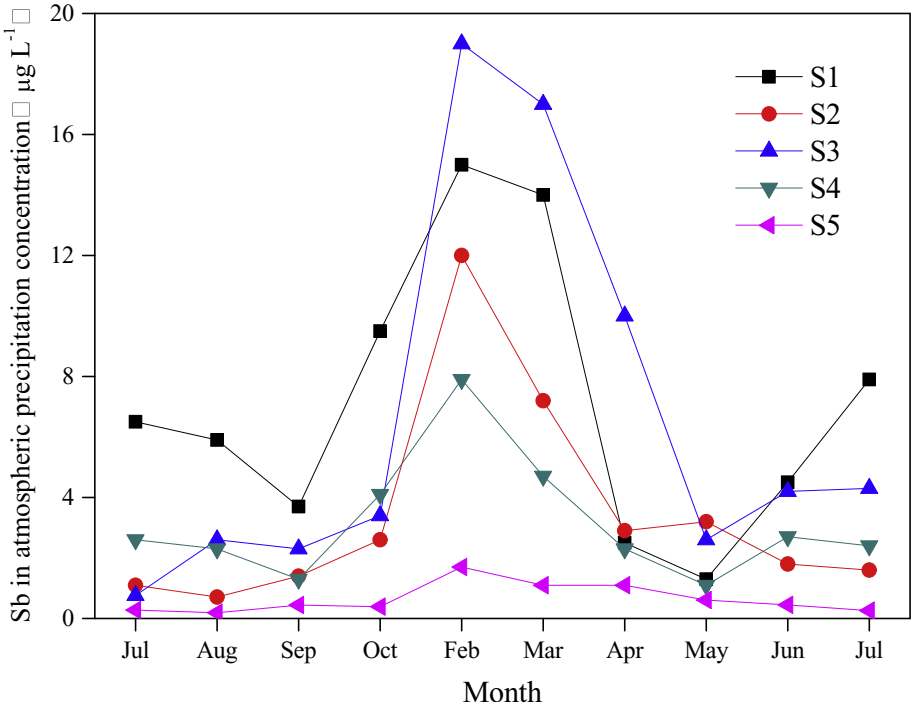

Fig. 2. Monthly variation of Sb concentrations in precipitation in Xunyang Hg–Sb mining district (S1–S4) and control site (S5).

3.2. Concentrations of Sb in soil

3.2.1. Concentrations of Sb in paddy soil

The concentrations and distribution of Sb in paddy soil in Xunyang Hg–Sb mining district is shown in Fig. 3. The average concentration of Sb in the paddy soil in the Xunyang Hg–Sb mining district was 584 ± 525 mg kg^{-1} (ranging from 25 to 1920 mg kg^{-1}). The concentration of Sb in paddy soil samples are consistently above the domestic environmental quality standard for agricultural soil (10 mg kg^{-1}, GB 15618–1995), showing that the rice paddy in Xunyang Hg–Sb mining district has been seriously polluted. As clearly shown in Fig. 3, the highest concentration of Sb in paddy soil was observed at 1#, which adjacent to the Hg–Sb smelter. The values decreased rapidly with the distance from the smelter. In addition, the Sb concentration in paddy soil adjacent to the Hg–Sb smelter (1#) was approximately 2 times higher than that near of Hg–Sb mine (5#), implying that the influence of the smelting activities on the surface soil is greater than the mining activities (Fig. 3).

3.2.2. Concentrations and variation of Sb in soil of experimental pots

The concentrations and variation of Sb in soil samples in the experimental pots during the period from June 2012 to June 2013 is summarized in Fig. 4. After 12 months exposure, the concentrations of Sb in soil of experimental pots at S1, S2, S3 and S4 were 29 ± 4.0 mg kg^{-1}, 7.5 ± 0.21 mg kg^{-1}, 6.8 ± 0.49 mg kg^{-1}, and 4.9 ± 0.38 mg kg^{-1} mg kg^{-1}, respectively, which were much higher than that at S5 (3.9 ± 0.15 mg kg^{-1}). As shown in Fig. 4, the concentrations of Sb in soil at S5 represented a narrow variation with time. More obvious temporal trend was observed at S1, S2, S3, and S4. The concentrations Sb in soil at S1, S2, S3, and S4 was low at the beginning of the sampling period (3.4 ± 0.09 mg kg^{-1}), but increased by factors of 8.5, 2.2, 2.0 and 1.2, respectively, after 12 months exposure. It is reasonable that the enhancement of Sb in soil of experimental pots at S1, S2, S3, and S4 exclusively attributed to the seriously Sb-contaminated air in the Xunyang Hg–Sb mining district.

The spatial distribution patterns of Sb in soil of experimental pots was similar to that of the rice paddy soil and precipitation in the Xunyang Hg–Sb mining district (Figs. 2 and 3). The highest concentration of Sb in soil was observed at S1, and then gradually decreased at S2, S3, and S4, respectively. During our sampling period, the Hg mining and smelting activities were ongoing. Specially, such processes without any pollution control on Sb resulted to serious Sb contamination to ambient atmosphere and then surface soil. Therefore, the consistent distribution patterns of Sb in precipitation, rice paddy soil, and experimental soil further confirmed that the atmospheric Sb deposition was the potential source of Sb to surface ecosystems in the Xunyang Hg–Sb mining district.

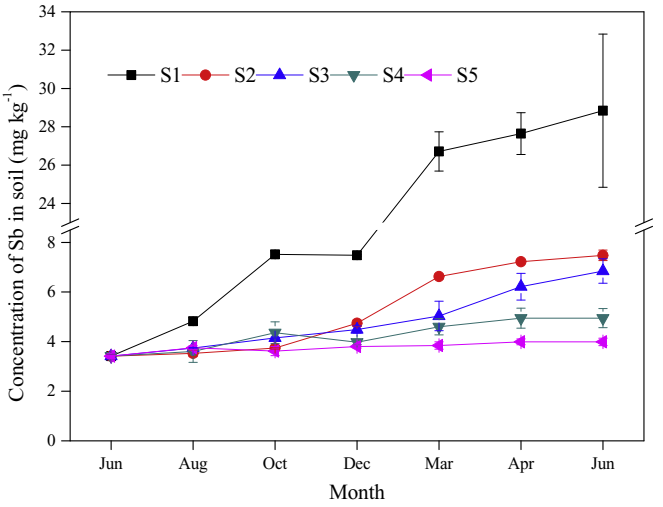

Fig. 4. Concentration of Sb in soil from experimental pots in the Xunyang Hg–Sb mining district and control site.

3.3. Atmospheric deposition of Sb

3.3.1. Wet deposition flux of Sb

The wet deposition flux of Sb in the Xunyang Hg–Sb mining district (S1–S4) and control sites (S5) were shown in Fig. 5. During the sampling period, the average (range) wet deposition fluxes of Sb at S1, S2, S3 and S4 were 13 ± 10 μg m^{-2} day^{-1} (3.8–36 μg m^{-2} day^{-1}), 5.4 ± 2.3 μg m^{-2} day^{-1} (2.1–9.3 μg m^{-2} day^{-1}), 9.8 ± 6.7 μg m^{-2} day^{-1} (4.2–27 μg m^{-2} day^{-1}) and 6.1 ± 3.6 μg m^{-2} day^{-1} (2.4–14 μg m^{-2} day^{-1}), respectively. Corresponding data was 1.3 ± 0.86 μg m^{-2} day^{-1} (0.54–2.9 μg m^{-2} day^{-1}) at control site of S5. The wet deposition flux of Sb in the Xunyang Hg–Sb mining

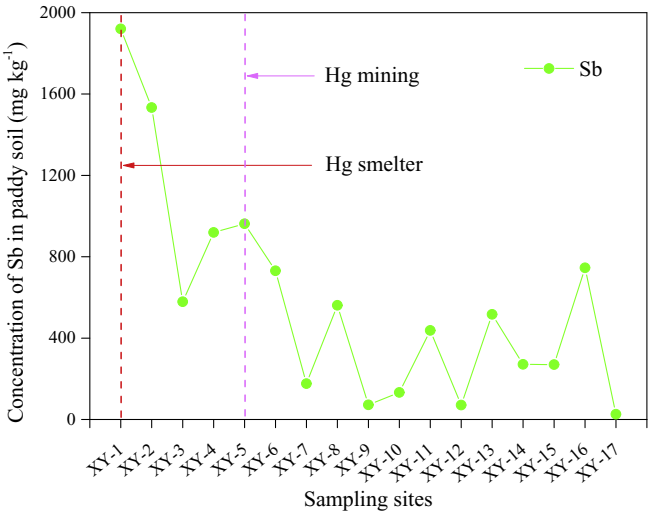

Fig. 3. Distribution of Sb concentrations in rice paddy soil in the Xunyang Hg–Sb mining district.

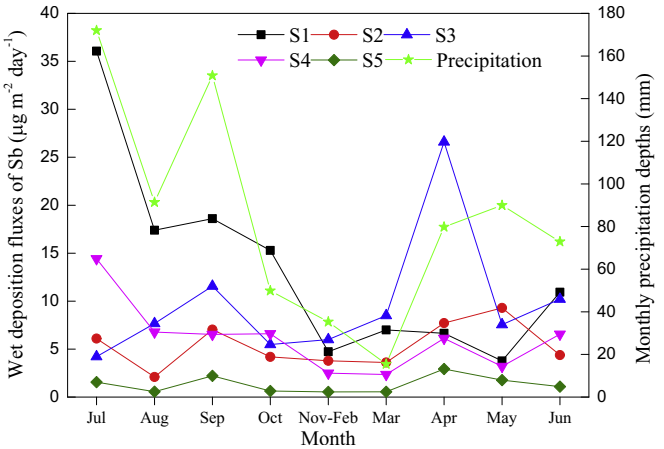

Fig. 5. Monthly changes in wet deposition fluxes of Sb at five sites and precipitations depths in the Xunyang Hg–Sb mining district.

district was 1–2 orders of magnitude higher than that in Shenzhen City (0.76 μg m^{-2} day^{-1}, Jiang et al., 2018), which is a typical industrial city in Southern China. However, the wet deposition flux of Sb at control site of S5 was much lower than Hong Kong (3.3 μg m^{-2} day^{-1}, Zheng et al., 2005) and Huelva (1.6–2.2 μg m^{-2} day^{-1}, Castillo et al., 2013), which are financial industries city in China and industrial estate in Spain, respectively. Most importantly, the wet deposition flux of Sb at control site of S5 was still relatively higher comparing with those of remote regions around the world, such as Noshiro (0.63 μg m^{-2} day^{-1}), Nakanoto (0.87 μg m^{-2} day^{-1}) and Matsuura (0.60 μg m^{-2} day^{-1}) of along the Japan Sea coast (Sakata and Asakura, 2009) and Amman in Jordan (0.12 μg m^{-2} day^{-1}, Al-Momani et al., 2008).

Relatively higher wet deposition fluxes generally occurred during the wet season compared to the dry season (Fig. 5), which accounted for 62% of the annual Sb wet deposition since the precipitation depths in wet season was 656.9 mm, with an average of 86.7% of the annual rainfall. Moreover, the wet deposition fluxes of Sb was much lower during the dry season (typically during November–April) compared to wet season, which was opposed to the Sb concentrations in precipitation between wet season and dry season (Fig. 2). Thus, the relatively lower wet deposition fluxes of Sb during dry season can be explained by the decreased rainfall rather than the Sb concentrations in precipitation. Previous study showed that wet deposition fluxes are generally higher for trace metals than dry deposition fluxes, which supports our observations (Al-Momani et al., 2008). Our results jointly with the previous study suggested that rain event and rainfall appeared to play an important role in atmospheric deposition of Sb in the Xunyang Hg–Sb mining district.

As shown in Fig. 5, the wet deposition flux of Sb in the Xunyang Hg–Sb mining district decreased with increasing distance from the smelter. The highest wet deposition flux of Sb was again observed at S1, which was adjacent to the smelter (Fig. 1). Similar to the distribution patterns of Sb concentration in precipitation (Fig. 2), the wet deposition flux of Sb in the Xunyang Hg–Sb mining district (S1–S4) was 1–2 orders of magnitude higher that at the control site of S5. Our results further confirmed that Sb emission from local smelter was predominant contribution to the Sb in surface soil layer in the Xunyang Hg–Sb mining district, while the control site of S5 was less impacted by the smelting activity. Furthermore, the spatial distribution of wet deposition flux of Sb implied that the effect of Sb emission through smelter on surface soil was limited in local region, but not in regional or global scale (>26 km, the distance between smelter and S5). Previous study suggested that coarse particles (>100 μm) show higher deposition rates due to sedimentation (Aléon et al., 2002), which agree with our observations and well explained the spatial distribution deposition flux of Sb in the Xunyang Hg–Sb mining district (S1–S4).

3.3.2. Dry deposition flux of Sb

The dry deposition flux of Sb in the Xunyang Hg–Sb mining district (S1–S4) and control sites (S5) were estimated. The mean (range) dry deposition fluxes of Sb at S1, S2, S3 and S4 were 4.9 ± 7.7 mg m^{-2} day^{-1} (0.044–20 mg m^{-2} day^{-1}), 0.80 ± 0.69 mg m^{-2} day^{-1} (0.14–2.0 mg m^{-2} day^{-1}), 0.76 ± 0.47 mg m^{-2} day^{-1} (0.38–1.6 mg m^{-2} day^{-1}) and 0.45 ± 0.49 mg m^{-2} day^{-1} (0.0086–1.3 mg m^{-2} day^{-1}), respectively. Corresponding data was 0.15 ± 0.16 mg m^{-2} day^{-1} (0.0041–0.42 mg m^{-2} day^{-1}) at control site of S5. The highest dry deposition flux of Sb was observed at S1, then gradually decreased with the distance from the smelter. In particular, the dry deposition fluxes of Sb at Xunyang Hg–Sb mining district were significantly higher than those for the wet deposition fluxes (T-test, $p < 0.01$).

3.3.3. Annual deposition mass of Sb

The total annual deposition mass of Sb in soil in the specific area of the Xunyang Hg–Sb mining district are summarized in Fig. 6. The annual deposition of Sb in the circle area of S1, S2, S3, S4 and S5 were 1.7 t y^{-1}, 17 t y^{-1}, 18 t y^{-1}, 43 t y^{-1}, and 80 t y^{-1}, respectively. The annual deposition mass of Sb was increased with the increasing distance from smelter (Fig. 6). Furthermore, the annual deposition mass of atmospheric Sb near the smelter was 1.7 t y^{-1}, and reached up to 80 t y^{-1} by 26 km distance (Fig. 6). As shown in Equation (4), the annual atmospheric deposition mass of Sb is related to the specific sub-area between the two adjacent experimental sites. Specially, for the sampling sites of S1, ΔA_1 (7.85×10^5 m^2) is the area within the S1 and the location of smelter, where the location of smelter and the distance between S1 and smelter are treated as the center and radius of the circle, respectively. For the sampling site of S5, ΔA_5 (1.67×10^9 m^2) is the ring area between S4 and S5, where the distance between S4 (S5) and smelter were treated as the radius of the circles. Although the concentrations of Sb in soil of experimental pots at S1 (29 ± 4.0 mg kg^{-1}) was much higher (7 times) than that at S5 (3.9 ± 0.15 mg kg^{-1}) after 12 months exposure, ΔA_5 was approximately 2128 times larger than that of ΔA_1, which resulted to the big difference in the annual Sb mass deposition between the sampling point close to the Hg smelter (S1) and the control point (S5). The deposition of Sb within 15 km radius, was occurs both through dry and wet deposition, whereas beyond 15 km wet deposition was the dominant pathway for Sb deposition (Telmer et al., 2004).

The annual wet deposition mass of Sb at S1, S2, S3, S4 and S5 were 0.0032 t y^{-1}, 0.088 t y^{-1}, 0.20 t y^{-1}, 0.64 t y^{-1}, and 0.67 t y^{-1} in the Xunyang Hg–Sb mining district, respectively. The corresponding annual dry deposition mass of Sb accounted for 98 ± 1.2% of the total annual deposition mass in the Xunyang Hg–Sb mining district. Our results suggested that the dry deposition flux was the predominant pathway for the removing the Sb in the atmosphere. Previous have reported that in regions with low precipitation (e.g. the Mediterranean climate area) dry deposition as a cleansing mechanism was more important than wet deposition on an annual basis (Muezzinoglu and Cizmecioglu, 2006). In contrast to the episodic nature of wet deposition, however, dry deposition was a continuous and dependable process involved in atmospheric cleansing (Grantz et al., 2003). Although wet deposition fluxes during precipitation events exceeded dry deposition fluxes by one to four orders of magnitude, dry deposition was nearly continuous (Lindberg and Harriss, 1981). Muezzinoglu and Cizmecioglu (2006) found that the wet deposition rates are more significant than the dry deposition rates on a daily basis; however, dry deposition is more important than wet deposition throughout the study period. Sakata et al. (2006) also showed that dry deposition rather than wet deposition is important for the deposition of several elements. Our result suggested that dry deposition to be a more important pathway for the removal of Sb from the atmosphere into the surface soil layer than wet deposition in the Xunyang Hg–Sb mining district, which was supported by previous studies (e.g. Grantz et al., 2003; Muezzinoglu and Cizmecioglu, 2006; Sakata et al., 2006).

The transport and deposition of atmospheric Sb are controlled by the prevailing wind in smelting operation area (Csavina et al., 2011; Li et al., 2017). Generally, westerly wind and the Asian monsoon provide warm humid southeast wind during wet seasons (summer and autumn); while cold dry northwest wind during dry seasons (spring and winter) dominate the large-scale wind system in the Xunyang Hg–Sb mining district (Fig. 1). The meteorological conditions during wet seasons (summer and autumn) are generally humid with abundant precipitation and dense vegetation, which may promote the deposition of atmospheric Sb in the Xunyang Hg–Sb mining district (Pan and Wang, 2015). However, the

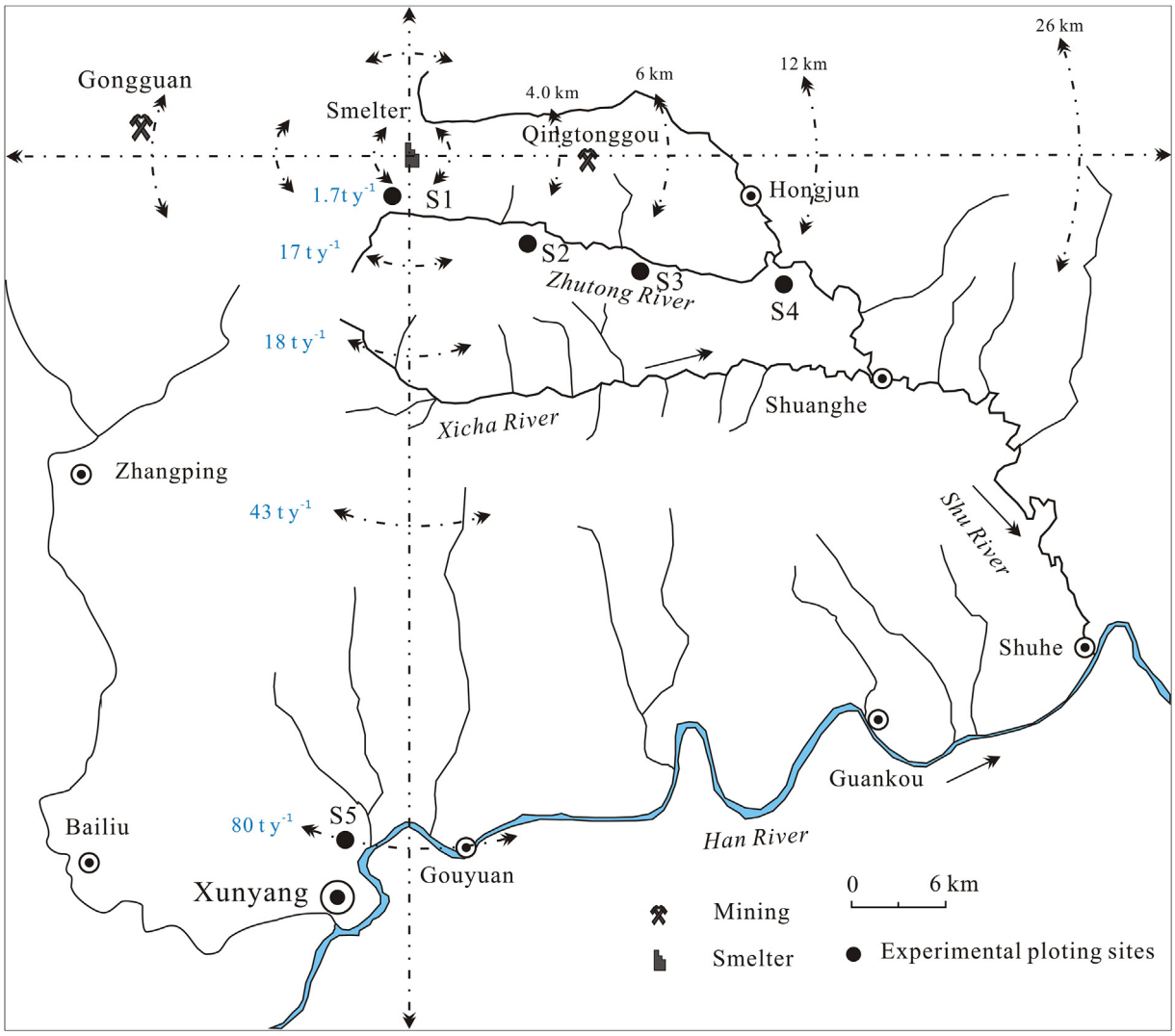

Fig. 6. Annual deposition mass of atmospheric Sb in the Xunyang Hg–Sb mining district (S1–S4) and control site (S5) (June 2012–June 2013).

relatively low precipitation jointly with the strong wind and the lack vegetation during dry seasons (spring and winter) may favor the re-suspension of soil particles to the atmosphere, resulting to the increased dry deposition of Sb in the study area (Chen et al., 2014). In addition, the topographic and physiographic characteristics are regarded as important factors controlling the prevalence of different air mass circulations (Castillo et al., 2013). The Xunyang Hg–Sb mining district is blocked by the Qinling Mountain. Therefore, the northwest wind associating with the channeling of airflows along the mountain valley are predominant during dry seasons (spring and winter) in the study area, which may stimulate the dry deposition of atmospheric Sb to the local terrestrial ecosystems.

Deposition of trace metals in areas surrounding emission sources, as well as "en route" deposition during transport, has reached levels in certain regions that have exceeded the maximum permissible values in soil and fresh water ecosystems (Pacyna and Pacyna, 2001). Among Asian countries, China is now regarded as the largest anthropogenic Sb emission source (He et al., 2012). The annual Sb emissions released from coal combustion in China increased from 133 t in 1980 to 546 t in 2007 (Tian et al., 2011). Nriagu and Pacyna (1988) estimated that global emissions of Sb into the atmosphere were 1400–5540 t y^{-1}, with anthropogenic sources of Sb emission being 10–18 times that of the natural source. Compared with global emissions, the Xunyang Hg–Sb mining district may pose a serious threat to the ecosystem and human health since the area has suffered such a high deposition fluxes of atmospheric Sb for a long time (Jones, 1994).

The atmospheric Sb signals observed from experimental soil reflect the contamination from the ongoing Hg–Sb smelting and mining activities in the Xunyang Hg–Sb mining district. Compared with previous observations (Krachler et al., 2005; He, 2007), such a high deposition mass of Sb in this study was mainly related to the production process of the Hg smelter. During the Hg–Sb mining activities, only Hg was recovered, while the Sb in the ore was directly released into the atmosphere or remain in waste residue, which resulted to the high Sb deposition mass to surface soil in the Xunyang Hg–Sb mining district. Our results indicated that the natural contributions to the total Sb inventory in surface soil could be negligible, and the anthropogenic emissions was the dominant atmospheric deposition of Sb in the Xunyang Hg–Sb mining district. Given that Sb-bearing aerosols from smelting processes are smaller than 1 μm, primarily in the form of relatively soluble oxides (Krachler et al., 2005), the serious Sb pollution in the Xunyang Hg–Sb mining district might have broader implications from human and ecosystem health risk and should be paid more attention.

This result raises important concerns regarding the potential effects of substantial metal deposition on different ecosystems. Therefore, it is important to further reduce the emissions to mitigate the environmental risks posed by atmospheric deposition in metal smelting area.

4. Conclusion

This study revealed serious contamination of Sb in precipitation and surface soil in the Xunyang Hg–Sb mining district, Shaanxi Province, Southwest China. The concentration of Sb in precipitation and paddy soil in the Xunyang Hg–Sb mining district were highly elevated compared to that in the control site; the highest values were observed near of the Hg–Sb smelter (0.5 km) and gradually decreased with the increase of distance from the smelter. The spatial distributions of Sb in precipitation and paddy soil implied that the ongoing Hg–Sb mining activities were the potential source of Sb to the atmosphere and soil in the Xunyang Hg–Sb mining district. The annual wet and dry deposition mass of Sb can reach up to 1.6 and 158 t y^{-1} in the Xunyang Hg–Sb mining district, respectively. Over 98% of atmospheric deposited Sb was presented as dry deposition, indicating that the dry deposition to be a more important pathway for the removal of Sb from the atmosphere into the surface soil layer than wet deposition. Current study confirmed that the ongoing Hg–Sb mining activities resulted to serious Sb contamination to surface terrestrial ecosystems, and posed a potential threat to local residents in the Xunyang Hg–Sb mining district.

Acknowledgements

This research was financially supported by the National Key R&D Program of China (No.2017YFD0800305) and Natural Science Foundation of China (U1612442, 41703130, 41473123, and 41673025).

References

Ainsworth, N., Cooke, J.A., Johnson, M.S., 1990. Distribution of antimony in contaminated grassland: 1-Vegetation and soils. Environ. Pollut. 65, 65–77. https://doi.org/10.1016/0269-7491(90)90165-9.

Aléon, J., Chaussidon, M., Marty, B., SchÜtz, L., Jaenicke, R., 2002. Oxygen isotopes in single micrometer-sized quartz grains: tracing the source of Saharan dust over long-distance atmospheric transport. Geochem. Cosmochim. Acta 66, 3351–3365. https://doi.org/10.1016/S0016-7037(02)00940-7.

Al-Momani, I.F., Momani, K.A., Jaradat, Q.M., Massadeh, A.M., Yousef, Y.A., Alomary, A.A., 2008. Atmospheric deposition of major and trace elements in Amman, Jordan. Environ. Monit. Assess. 136 (1–3), 209–218. https://doi.org/10.1007/s10661-007-9676-4.

Al-Momani, I.F., 2008. Wet and dry deposition fluxes of inorganic chemical species at a rural site in northern Jordan. Arch. Environ. Contam. Toxicol. 55 (4), 558–565. https://doi.org/10.1007/s00244-008-9148-z.

Bloch, P., Vanderborght, B., Adams, F., Land, J.V., 1983. Investigation of the emissions of an antimony metallurgical factory with transmission electron microscopy. Int. J. Environ. Anal. Chem. 14, 257–274. https://doi.org/10.1080/03067318308071624.

Castillo, S., Rosa, J.D.D.L., Campa, A.M.S.D.L., González-Castanedo, Y., Fernández-Camacho, R., 2013. Heavy metal deposition fluxes affecting an Atlantic coastal area in the southwest of Spain. Atmos. Environ. 77 (3), 509–517. https://doi.org/10.1016/j.atmosenv.2013.05.046.

Chate, D.M., Rao, P., Naik, M.S., Momin, G.A., Safai, P.D., Ali, K., 2003. Scavenging of aerosols and their chemical species by rain. Atmos. Environ. 37 (18), 2477–2484. https://doi.org/10.1016/S1352-2310(03)00162-6.

Chen, Y., Schleicher, N., Chen, Y., Chai, F.H., Norra, S., 2014. The influence of governmental mitigation measures on contamination characteristics of PM(2.5) in Beijing. Sci. Total Environ. 490, 647–658. https://doi.org/10.1016/j.scitotenv.2014.05.049.

Cloy, J.M., Farmer, J.G., Graham, M.C., MacKenzie, A.B., Cook, G.T., 2005. A comparison of antimony and lead profiles over the past 2500 years in flanders moss ombrotrophic peat bog, Scotland. J. Environ. Monit. 7, 1137–1147. https://doi.org/10.1039/b510987f.

Csavina, J., Landázuri, A., Wonaschütz, A., Rine, K., Rheinheimer, P., Barbaris, B., Betterton, E.A., 2011. Metal and metalloid contaminants in atmospheric aerosols from mining operations. Water, Air, Soil Pollut. 221 (1–4), 145–157. https://doi:10.1007/s11270-011-0777-x.

Ferrat, M., Weiss, D.J., Dong, S., Large, D.J., Spiro, B., Sun, Y.B., Gallagher, K., 2012. Lead atmospheric deposition rates and isotopic trends in Asian dust during the last 9.5 kyr recorded in an ombrotrophic peat bog on the eastern Qinghai-Tibetan Plateau. Geochem. Cosmochim. Acta 82, 4–22. https://doi.org/10.1016/j.gca.2010.10.031.

Filella, M., Belzile, N., Chen, Y.W., 2002. Antimony in the environment: a review focused on natural waters: I. Occurrence. Earth Sci. Rev. 57, 125–176. https://doi.org/10.1016/S0012-8252(01)00070-8.

Filella, M., Williams, P.A., Belzile, N., 2016. Antimony in the environment: knowns and unknowns. Environ. Chem. 6, 95–105. https://doi.org/10.1071/EN09007.

Graedel, T.E., Franey, J.P., 1975. Field measurements of submicron aerosol washout by snow. Geophys. Res. Lett. 2, 325–328. https://doi.org/10.1029/GL002i008p00325.

Grantz, D.A., Garner, J.H., Johnson, D.W., 2003. Ecological effects of particulate matter. Environ. Int. 29 (2), 213–239. https://doi.org/10.1016/S0160-4120(02)00181-2.

Guentzel, J.L., Landing, W.M., Gill, G.A., Pollman, C.D., 1995. Atmospheric deposition of mercury in Florida: The fams project (1992-1994). Water. Air. Soil. Poll 80 (1-4), 393–402. https://doi.org/10.1007/bf01189689.

Guentzel, J.L., Landing, W.M., Gill, G.A., Poliman, C.D., 2001. Processes influencing rainfall deposition of mercury in Florida. Environ.Sci.Technol 35, 863–873. https://doi.org/10.1021/es001523.

Guo, Y.N., Feng, X.B., Li, Z.G., He, T.R., Yan, H.Y., Meng, B., Zhang, J.F., Qiu, G.L., 2008. Distribution and wet deposition fluxes of total and methyl mercury in Wujiang River Basin, Guizhou, China. Atmos. Environ. 42, 7096–7103. https://doi.org/10.1016/j.atmosenv.2008.06.006.

Hammel, W., Debus, R., Steubing, L., 2000. Mobility of antimony in soil and its availability to plants. Chemosphere 41, 1791–1798. https://doi.org/10.1016/S0045-6535(00)00037-0.

He, M.C., Yang, J., 1999. Effects of different forms of antimony on rice during the period of germination and growth and antimony concentration in rice tissue. Sci. Total Environ. s 243–244, 149–155. https://doi.org/10.1016/S0048-9697(99)00370-8.

He, M.C., 2007. Distribution and phytoavailability of antimony at an antimony mining and smelting area, Hunan, China. Environ. Geochem. Health 29, 209–219. https://doi.org/10.1007/s10653-006-9066-9.

He, M.H., Wang, X.Q., Wu, F.C.C., Fu, Z.Y., 2012. Antimony pollution in China. Sci. Total. Environ 421–422 (3), 41–50. https://doi.org/10.1016/j.scitotenv.2011.06.009.

Hu, X.W., Murao, S., Shi, M.K., Li, B., 1996. Classification and distribution of antimony deposits in China. Resour. Geol. 46, 287–297. https://doi.org/10.11456/shigenchishitsu1992.46.287.

Huston, R., Chan, Y.C., Chapman, H., Gardner, T., Shaw, G., 2012. Source apportionment of heavy metals and ionic contaminants in rainwater tanks in a sub-tropical urban area in Australia. Water Res. 46, 1121–1132. https://doi.org/10.1016/j.watres.2011.12.008.

Jiang, B.Y., He, L., Chen, D.H., Gu, T.A., Liang, Z.W., Wang, M.J., Wang, X.Y., Li, S.A., 2018. Wet deposition flux and sources of heavy metals in precipitation in the coastal area of Shenzhen. Environ. Chem. 37 (7), 1460–1473 (In Chinese). https://doi.org/10.7524/j.issn.0254-6108.2017091901.

Jones, R.D., 1994. Survey of antimony workers: mortality 1961-1992. Occup. Environ. Med. 51, 772–776. https://doi.org/10.1136/oem.51.11.772.

Kentner, M., Leinemann, M., Schaller, K.H., Weltle, D., Lehnert, G., 1995. External and internal antimony exposure in starter battery production. Int. Arch. Occup. Environ. Health 67, 119–123. https://doi.org/10.1007/BF00572235.

Krachler, M., Zheng, J., Koerner, R., Zdanowicz, C., Fisher, D., Shotyk, W., 2005. Increasing atmospheric antimony contamination in the northern hemisphere: snow and ice evidence from Devon Island, Arctic Canada. J. Environ. Monit. 7, 1169–1176. https://doi.org/10.1039/b509373b.

Landing, W.M., Guentzel, J.L., Gill, G.A., Pollman, C.D., 1998. Methods for measuring mercury in rainfall and aerosols in Florida. Atmos. Environ. 32 (5), 909–918. https://doi.org/10.1016/s1352-2310(97)00115-5.

Landis, M.S., Keeler, G.J., 1997. Critical evaluation of a modified automatic wet-only precipitation collector for mercury and trace element determinations. Environ. Sci. Technol 31 (9), 2610–2615. https://doi.org/10.1021/es9700055.

Li, Y.M., Pan, Y.P., Wang, Y.S., Wang, Y.F., Li, X.R., 2012. Chemical characteristics and sources of trace metals in precipitation collected from a typical industrial city in Northern China. Environ. Sci. 33, 3712–3717 (in Chinese). https://doi.org/10.13227/j.hjkx.2012.11.018.

Li, X., Yang, H., Zhang, C., Zeng, G.M., Liu, Y.G., Xu, W.H., Wu, Y.E., Lan, S.M., 2017. Spatial distribution and transport characteristics of heavy metals around an antimony mine area in central China. Chemosphere 170, 17–24. https://doi.org/10.1016/j.chemosphere.2016.12.011.

Lindberg, S.E., Harriss, R.C., 1981. The role of atmospheric deposition in an eastern U.S. deciduous forest. Water Air Soil Pollut. 16 (1), 13–31. https://doi.org/10.1007/bf01047039.

Meima, J.A., Comans, R.N.J., 1998. Reducing Sb-leaching from municipal solid waste incinerator bottom ash by addition of sorbent minerals. J. Geochem. Explor. 62, 299–304. https://doi.org/10.1016/S0375-6742(97)00044-7.

Muezzinoglu, A., Cizmecioglu, S.C., 2006. Deposition of heavy metals in a Mediterranean climate area. Atmos. Res. 81 (1), 1–16. https://doi.org/10.1016/j.atmosres.2005.10.004.

Nakamaru, Y., Tagami, K., Uchida, S., 2006. Antimony mobility in Japanese

agricultural soils and the factors affecting antimony sorption behavior. Environ. Pollut. 141, 321–326. https://doi.org/10.1016/j.envpol.2005.08.040.
Nriagu, J.O., Pacyna, J.M., 1988. Quantitative assessment of worldwide contamination of air, water and soils by trace metals. Nature 333, 134–139. https://doi.org/10.1038/333134a0.
Nriagu, J.O., 1989. A global assessment of natural sources of atmospheric trace metals. Nature 338, 47–49. https://doi.org/10.1038/338047a0.
Pacyna, J.M., Pacyna, E.G., 2001. An assessment of global and regional emissions of trace metals to the atmosphere from anthropogenic sources worldwide. Environ. Rev. 9, 269–298. https://doi.org/10.1139/a01-012.
Pan, Y.P., Wang, Y.S., 2015. Atmospheric wet and dry deposition of trace elements at 10 sites in Northern China. Atmos. Chem. Phys. 14 (2), 951–972. https://doi.org/10.5194/acp-15-951-2015.
Qiu, G.L., Feng, X.B., Meng, B., Sommar, J., Gu, C.H., 2012. Environmental geochemistry of an active Hg mine in Xunyang, Shaanxi province, China. Appl. Geochem. 27, 2280–2288. https://doi.org/10.1016/j.apgeochem.2012.08.003.
Sakata, M., Marumoto, K., Narukawa, M., Asakura, K., 2006. Regional variations in wet and dry deposition fluxes of trace elements in Japan. Atmos. Environ. 40 (3), 521–531, 2006. https://doi.org/10.1016/j.atmosenv.2005.09.066.
Sakata, M., Asakura, K., 2009. Factors contributing to seasonal variations in wet deposition fluxes of trace elements at sites along Japan Sea coast. Atmos. Environ. 43 (25), 3867–3875. https://doi.org/10.1016/j.atmosenv.2009.05.001.
Schnorr, T.M., Steenland, K., Thun, M.J., Rinsky, R.A., 1995. Mortality in a cohort of antimony smelter workers. Am. J. Ind. Med. 27, 59–770. https://doi.org/10.1002/ajim.4700270510.
Shimamura, T., Wada, T., Iwashita, M., Takaku, Y., Ohashi, H., 2006. Scavenging properties of major and trace species in rainfall collected in urban and suburban Tokyo. Atmos. Environ. 40 (22), 4220–4227. https://doi.org/10.1016/j.atmosenv.2006.03.010.
Shotyk, W., Krachler, M., Chen, B., 2004. Antimony in recent, ombrotrophic peat from Switzerland and Scotland: comparison with natural background values (5,320 to 8,020 14C yr BP) and implications for the global atmospheric Sb cycle. Global Biogeochem. Cycles 18, 1–13. https://doi.org/10.1029/2003GB002113.
Smichowski, P., 2008. Antimony in the environment as a global pollutant: a review on analytical methodologies for its determination in atmospheric aerosols. Talanta 75, 2–14. https://doi.org/10.1016/j.talanta.2007.11.005.
Telmer, K., Bonham-Carter, G.F., Kliza, D.A., Hall, G.E.M., 2004. The atmospheric transport and deposition of smelter emissions: evidence from the multi-element geochemistry of snow, Quebec, Canada 1. Geochem. Cosmochim. Acta 68, 2961–2980. https://doi.org/10.1016/j.gca.2003.12.022.
Tian, H.Z., Zhao, D., He, M.C., Wang, Y., Cheng, K., 2011. Temporal and spatial distribution of atmospheric Sb emission inventories from coal combustion in China. Environ. Pollut. 159, 1613–1619. https://doi.org/10.1016/j.envpol.2011.02.048.
Tian, H.Z., Zhou, J.R., Zhu, C.Y., Zhao, D., Gao, J.J., Hao, J.M., He, M.C., Liu, K.Y., Wang, K., Hua, S.B., 2014. A comprehensive global inventory of atmospheric Sb emissions from anthropogenic activities, 1995-2010. Environ. Sci. Technol. 48, 10235–10241. https://doi.org/10.1021/es405817u.
Tighe, M., Lockwood, P., Wilson, S., 2005. Adsorption of antimony (V) by floodplain soils, amorphous iron (III) hydroxide and humic acid. J. Environ. Monit. 7, 1177–1185. https://doi.org/10.1039/b508302h.
Wang, H., Ma, N., Yang, X.J., Yang, K.M., Han, G.L., 2010. The characteristic of metals in precipitation collected from Chengdu, China. Earth. Environ. 38, 49–53 (In Chinese). https://doi.org/10.14050/j.cnki.1672-9250.2010.01.011.
Wedepohl, K.H., 1995. The composition of the continental crust. Geochem. Cosmochim. Acta 59, 1217–1232. https://doi.org/10.1016/0016-7037(95)00038-2.
WHO, 1996. Guidelines for Drinking-water Quality: Volume 2. Health Criteria and Other Supporting Information, second ed. World Health Organization, Geneva, p. 937. 1996.
Wilson, N.J., Craw, D., Hunter, K., 2004. Antimony distribution and environmental mobility at an historic antimony smelter site, New Zealand. Environ. Pollut. 129 (2), 257–266. https://doi:10.1016/j.envpol.2003.10.014.
Wilson, S.C., Lockwood, P.V., Ashley, P.M., Tighe, M., 2010. The chemistry and behaviour of antimony in the soil environment with comparisons to arsenic: a critical review. Environ. Pollut. 158, 1169–1181. https://doi.org/10.1016/j.envpol.2009.10.045.
Zhang, G.P., Liu, C.Q., Liu, H., Hu, J., Han, G.L., Li, L., 2009a. Mobilisation and transport of arsenic and antimony in the adjacent environment of Yata gold mine, Guizhou Province, China. J. Environ. Monit. 11, 1570–1578. https://doi.org/10.1039/b908612a.
Zhang, L., Jin, Y.Q., Lu, J.L., Zhang, C.X., 2009b. Concentration, distribution and bioaccumulation of mercury in the Xunyang mercury mining area, Shaanxi Province, China. Appl. Geochem. 24, 950–956. https://doi.org/10.1016/j.apgeochem.2009.02.027.
Zheng, J., Ohata, M., Furuta, N., 2000. Studies on the speciation of inorganic and organic antimony compounds in airborne particulate matter by HPLC-ICP-MS. Analyst 125 (6), 1025–1028. https://doi.org/10.1039/b002201m.
Zheng, M., Guo, Z., Fang, M., Rahn, K.A., Kester, D.R., 2005. Dry and wet deposition of elements in Hong Kong. Mar. Chem. 97 (1–2), 124–139. https://doi.org/10.1016/j.marchem.2005.05.007.